

# Optimized Vectorization Implementation of CRYSTALS-Dilithium

Jieyu Zheng, Haoliang Zhu, Zhenyu Song, Zheng Wang, Yunlei Zhao

**Abstract**—CRYSTALS-Dilithium is a lattice-based signature scheme to be standardized by NIST as the primary post-quantum signature algorithm. In this work, we make a thorough study of optimizing the implementations of Dilithium by utilizing the Advanced Vector Extension (AVX) instructions, specifically AVX2 and the latest AVX512.

We first present an improved parallel small polynomial multiplication with tailored early evaluation (PSPM-TEE) to further speed up the signing procedure, which results in a speedup of 5%-6% compared with the original PSPM Dilithium implementation. We then present a tailored reduction method that is simpler and faster than Montgomery reduction. Our optimized AVX2 implementation exhibits a speedup of 3%-8% compared with the state-of-the-art of Dilithium AVX2 software. Finally, for the first time, we propose a fully and highly vectorized implementation of Dilithium using AVX-512. This is achieved by carefully vectorizing most of Dilithium functions with the AVX512 instructions in order to improve efficiency both for time and for space simultaneously.

With all the optimization efforts, our AVX-512 implementation improves the performance by 37.3%/50.7%/39.7% in key generation, 34.1%/37.1%/42.7% in signing, and 38.1%/38.7%/40.7% in verification for the parameter sets of Dilithium2/3/5 respectively. To the best of our knowledge, our AVX512 implementation has the best performance for Dilithium on the Intel x64 CPU platform to date.

**Index Terms**—Post-Quantum Cryptography, Lattice-Based Cryptography, CRYSTALS-Dilithium, AVX2, AVX-512, Software Optimization.

## I. INTRODUCTION

WITH the popularity of authentication and non-repudiation, it is more common to construct digital signatures using asymmetric cryptographic techniques. Currently, millions of web servers use digital signatures as part of Transport Level Security (TLS) [1]–[3], which allows users to verify the server’s identity. Both hardware and software vendors rely on digital signatures to guarantee entity integrity. Digital signatures are also essential for cybersecurity infrastructure. Most of the current digital signatures are implemented based on Rivest-Shamir-Adleman (RSA) [4], Elliptic Curve Cryptography (ECC), or Digital Signature Algorithm (DSA).

However, in the era of continuous development of quantum computers, traditional public key cryptography and DSA appear to be in jeopardy. Using Shor’s algorithm [5], an attacker with a powerful quantum computer can obtain the corresponding private key in polynomial time by analyzing the public key of RSA or ECC. The National Institute of Standards and Technology (NIST) proposed in [6] that by 2030 an RSA 2048-bit key may be broken by a quantum computer within a few hours. As a result, NIST has launched a competition

to solicit standard algorithms for PQC, including soliciting and evaluating quantum-resistant secure digital signature algorithms. On July 5th 2022, NIST announced the first algorithms to be standardized. There are three signature schemes selected: CRYSTALS-Dilithium, FALCON and SPHINCS+ [7], among them CRYSTALS-Dilithium is recommended by NIST as the primary signature algorithm to be used. CRYSTALS-Dilithium is a digital signature scheme based on lattice theory, whose security is based on the Module Learning With Errors (MLWE) [8] and the Module Short Integer Solution (MSIS) [9] problems. Most of the operations of Dilithium are based on the cyclotomic polynomial ring arithmetic. Number Theoretic Transform (NTT) is a common technique used to speed up polynomial multiplication. Dilithium scheme uses the Fiat-Shamir with Aborts structure [10]. So the signature process will reject sampling through a series of conditional checks to ensure that the generated signature will not leak private key information.

NIST chose the 64-bit Intel architecture (i.e. x64) as the main benchmarking platform of NIST PQC candidates. Advanced Vector Extension (AVX) is x64 Intel architecture instruction set [11]. The first AVX instruction is proposed by Intel in 2008. AVX-512 is the newest version of Intel Advanced Vector eXtensions [12]. It has 32 512-bit vector registers called *zmm* registers. The vector registers are divided into different data lanes. Instructions are operated in-lane simultaneously. AVX-512 instruction set can accelerate the non-sequential process with the best performance among all AVX serial instruction sets, for its registers with maximum data width. The parallelism of AVX-512 is based on the “Single Instruction Multiple Data (SIMD)” idea. AVX-512 provides various permutation instructions and masked loads/stores that are especially efficient to implement hash functions, NTT, and rejection sampling. AVX-512IFMA has the potential to speed up multiply and add operations.

a) *Related Work*: The optimization work of Dilithium includes software optimization implementation and hardware optimization implementation. In this paper, we focus on the software-optimized implementation of Dilithium. There are a list of software implementations related to Dilithium. The basic software implementation is the C REF implementation that the CRYSTALS team submitted to NIST [13]. However, the C REF implementation is not optimized and has lower efficiency. Additionally, the CRYSTALS team provided a faster AVX2 optimized version [13] on x64 CPUs. Recently, software optimization studies mainly focus on CPU/GPU environments and embedded systems like ARM. Ravi et al. [14] presented a signed polynomial representation implementation

for Cortex-M4 and proposed various stack consumptions and speed trade-offs for the signing procedure. Kim et al. [15] presented a method for designing the NTT multiplications of CRYSTALS-Dilithium using advanced SIMD instructions and vector registers. “Asymmetric multiplication” for matrix-to-vector polynomial multiplication was introduced in [16]. Abdulrahman et al. [17] proposed to switch to a smaller prime modulus for small polynomial multiplication in the signing procedure of Dilithium. [18] presented optimizations of Dilithium on IBM z15 architecture, and mentioned that employing some optimization methods with advanced instruction sets like AVX-512 as future work. Zheng et al. [19] presented a parallel small polynomial multiplication (PSPM) algorithm that can fastly compute small vector polynomial multiplication in Dilithium, based on which the C and ARM Neon implementation were proposed.

For AVX-512 implementations of PQC algorithms, some arithmetics like large integer multiplication, Montgomery multiplication, and NTT AVX-512 implementation have received researchers’ attention [20]–[25]. Cheng et al. [26] proposed a highly vectorized implementation for SIKE. [27] presented an implementation using AVX-512 to batch CSIDH group actions. [28] presented an implementation using AVX-512 for SPHINCS+. Cabral et al. [29] presented an optimized AVX-512 implementation for SHA-3 family. Up till now, to the best of our knowledge, there is still no AVX-512 optimized implementation for Dilithium. It’s also interesting to investigate whether the current state-of-art of AVX2 implementations for Dilithium can be further improved.

*b) Contribution:* Our contribution is summarized as follows.

- 1) We present an improved parallel small polynomial multiplication with tailored early evaluation (PSPM-TEE) to further speed up the signing procedure. We implement this algorithm using both C, AVX2, and AVX-512.
- 2) We present a tailored reduction method that is faster than Montgomery reduction, and apply it to the first level of  $\text{NTT}(t_0)$ ,  $\text{NTT}(t_1)$  for Dilithium2/3/5 and  $\text{NTT}(y)$  for Dilithium2.
- 3) We propose an optimized implementation of the tailored reduction, consisting of only two instructions and utilizing AVX-512IFMA, which results in the reduction of one instruction and two cycle counts compared to the implementation using AVX-512F. In comparison to Montgomery reduction, the tailored reduction using AVX-512IFMA offers a more efficient performance, saving up to two instructions and six cycle counts.
- 4) We present optimized AVX2 implementation of Dilithium by integrating our improved PSPM-TEE, tailored reduction, and lazy reduction techniques. Our optimized AVX2 implementation exhibits a speedup of 3%-8% compared with the state-of-the-art of Dilithium AVX2 software.
- 5) For the first time, we propose a fully and highly vectorized implementation of Dilithium using AVX-512. We carefully vectorize most of Dilithium functions, especially performance bottlenecks including  $\text{NTT}$ ,  $\text{NTT}^{-1}$ , Montgomery reduction, hashing, and parallel reject

sampling. In particular, we present a space-efficient implementation of parallel rejection sampling using AVX-512 without a big precomputation table, as otherwise the space consumption is infeasible by applying the implementation method using AVX2. With all these optimization efforts, our AVX-512 implementation improves the performance by 37.3%/50.7%/39.7% in key generation, 34.1%/37.1%/42.7% in signing, and 38.1%/38.7%/40.7% in verification for the parameter sets of Dilithium2/3/5 respectively. To the best of our knowledge, our AVX512 implementation achieves the best performance for Dilithium on the Intel x64 CPU platform thus far.

*c) Code:* We will later open source our code.

*d) Structure of this paper:* This paper is organized as follows. Section II reviews some preliminaries. Section III presents an improved PSPM with early evaluation. Section IV introduces the proposed special Tailored reduction. Section V deals with the AVX-512 implementation of Dilithium and presents various optimization strategies. In Section VI we go through the performance results and comparison.

## II. PRELIMINARIES

### A. Notation

We denote polynomials by lowercase Latin letter  $c$  (the coefficient of a polynomial is  $c_i$ , which represents the  $i$ -th element of  $c$ ), vectors of polynomials by bold lowercase letter  $\mathbf{t}$ , and matrices by bold upper case letter  $\mathbf{A}$ . If they are transformed to NTT-domain, then we add a hat to make a tag, e.g.,  $\hat{c}$ ,  $\hat{\mathbf{t}}$  and  $\hat{\mathbf{A}}$ .

Let  $\mathbb{Z}_q \stackrel{\text{def}}{=} \mathbb{Z}/q\mathbb{Z}$ ,  $\mathcal{R} \stackrel{\text{def}}{=} \mathbb{Z}[x]/(x^n + 1)$ , and  $\mathcal{R}_q \stackrel{\text{def}}{=} \mathbb{Z}_q[x]/(x^n + 1)$ . Element  $a_i \in \mathbb{Z}_q$  will be represented by one element in  $\{-\frac{q-1}{2}, \dots, 0, \dots, \frac{q-1}{2}\}$ . Polynomial  $a \in \mathcal{R}_q$  can be represented by  $a = \sum_{i=0}^{n-1} a_i \cdot x^i$ , where  $a_i \in \mathbb{Z}_q$ .

The operator  $\circ$  denotes coefficient-wise multiplication. The operator  $\parallel$  concatenates two inputs into a byte stream. For  $a_i \in \mathbb{Z}_q$ ,  $\|a_i\|_\infty$  denotes  $|a_i \bmod \pm q|$  (the absolute value of  $(a_i \bmod \pm q)$ ). For a finite set  $S$  or a distribution  $D$ ,  $x \leftarrow S$  denotes random sampling of an element from the set  $S$ , and  $x \leftarrow D$  denotes sampling  $x$  according to distribution  $D$ .  $\lfloor z \rfloor$  means rounding down  $z$  and  $\lceil z \rceil$  means rounding to the nearest integer of  $z$ .

### B. CRYSTALS-Dilithium Signature Scheme

CRYSTALS-Dilithium is a post-quantum digital signature algorithm based on the hardness of MSIS and MLWE lattice problems. Algorithm 1, 2, and 3 specify the CRYSTALS-Dilithium key generation, signature generation, and signature verification, respectively. The polynomial ring in Dilithium is  $\mathbb{Z}_q[x]/(x^n + 1)$ , where  $n = 256$ ,  $q = 8380417$ .

The function `NumberOfOne` means to count the number of 1’s in a vector of polynomials. For the details about the seed expansion functions `ExpandA`, `ExpandS` and `ExpandMask`, the rounding functions `Power2Round`, `HighBits`, `LowBits` and `Decompose`, and the hint functions `MakeHint` and `UseHint`, the

generating  $c$  polynomial function `SampleInBall`, the reader can refer to the Dilithium specification [30].

---

**Algorithm 1** Dilithium.KeyGen()

---

**Input:**  $\zeta \leftarrow \{0, 1\}^{256}$   
**Output:** Public and secret keys  
 $(pk = (\rho, \mathbf{t}_1), sk = (\rho, K, tr, \mathbf{s}_1, \mathbf{s}_2, \mathbf{t}_0))$   
1:  $(\rho, \rho', K) \in \{0, 1\}^{256} \times \{0, 1\}^{512} \times \{0, 1\}^{256} := H(\zeta)$   $\triangleright$   $H$  is instantiated as SHAKE-256  
2:  $\mathbf{A} \in \mathcal{R}_q^{k \times \ell} := \text{ExpandA}(\rho)$   $\triangleright$   $\mathbf{A}$  is generated and stored in NTT Representation as  $\hat{\mathbf{A}}$   
3:  $(\mathbf{s}, \mathbf{e}) \in S_\eta^\ell \times S_\eta^k := \text{ExpandS}(\rho')$   
4:  $\mathbf{t} := \mathbf{A}\mathbf{s} + \mathbf{e}$   $\triangleright$  Compute  $\mathbf{A}\mathbf{s}$  as  $\text{NTT}^{-1}(\hat{\mathbf{A}} \circ \text{NTT}(\mathbf{s}))$   
5:  $(\mathbf{t}_1, \mathbf{t}_0) := \text{Power2Round}_{q,d}(\mathbf{t})$   
6:  $tr \in \{0, 1\}^{256} := H(\rho \parallel \mathbf{t}_1)$   
7: **return**  $(pk = (\rho, \mathbf{t}_1), sk = (\rho, K, tr, \mathbf{s}, \mathbf{e}, \mathbf{t}_0))$

---

### C. Hashing

The hash functions used by Dilithium are two eXtensible Output Functions (XOF), namely SHAKE-256 and SHAKE-128 [31]. XOF maps an arbitrary-length bit string to a string of infinitely many bits. Dilithium uses these XOF functions mainly for generating random bytes of SHAKE-128 to sample matrix  $\mathbf{A}$  and for generating random bytes of SHAKE-256 to sample  $\mathbf{s}$ ,  $\mathbf{e}$  and  $\mathbf{y}$ .

---

**Algorithm 2** Dilithium.Sign( $sk, M$ )

---

**Input:** Secret key  $sk = (\rho, K, tr, \mathbf{s}, \mathbf{e}, \mathbf{t}_0)$ , Message  $M \in \{0, 1\}^*$   
**Output:** Signature  $\sigma = (\tilde{c}, \mathbf{z}, \mathbf{h})$   
1:  $\mathbf{A} \in \mathcal{R}_q^{k \times \ell} := \text{ExpandA}(\rho)$   $\triangleright$   $\mathbf{A}$  is generated and stored in NTT Representation as  $\hat{\mathbf{A}}$   
2:  $\mu \in \{0, 1\}^{512} := H(tr \parallel M)$   
3:  $\kappa := 0, (\mathbf{z}, \mathbf{h}) := \perp$   
4:  $\rho' \in \{0, 1\}^{512} := H(K \parallel \mu)$  (or  $\rho' \leftarrow \{0, 1\}^{512}$  for randomized signing)  
5: **while**  $(\mathbf{z}, \mathbf{h}) = \perp$  **do**  $\triangleright$  Pre-compute  
 $\hat{\mathbf{s}}_1 := \text{NTT}(\mathbf{s}), \hat{\mathbf{e}}_2 := \text{NTT}(\mathbf{e}),$  and  $\hat{\mathbf{t}}_0 := \text{NTT}(\mathbf{t}_0)$   
6:  $\mathbf{y} \in \tilde{S}_{\gamma_1}^\ell := \text{ExpandMask}(\rho', \kappa)$   
7:  $\mathbf{w} := \mathbf{A}\mathbf{y}$   $\triangleright \mathbf{w} := \text{NTT}^{-1}(\hat{\mathbf{A}} \circ \text{NTT}(\mathbf{y}))$   
8:  $\mathbf{w}_1 := \text{HighBits}_q(\mathbf{w}, 2\gamma_2)$   
9:  $\tilde{c} \in \{0, 1\}^{256} := H(\mu \parallel \mathbf{w}_1)$   
10:  $c \in B_\tau := \text{SampleInBall}(\tilde{c})$   $\triangleright$  Store  $c$  in NTT representation as  $\hat{c} = \text{NTT}(c)$   
11:  $\mathbf{z} := \mathbf{y} + c\mathbf{s}$   $\triangleright$  Compute  $c\mathbf{s}$  as  $\text{NTT}^{-1}(\hat{c} \circ \hat{\mathbf{s}})$   
12:  $\mathbf{r}_0 := \text{LowBits}_q(\mathbf{w} - c\mathbf{e}, 2\gamma_2)$   $\triangleright$  Compute  $c\mathbf{e}$  as  $\text{NTT}^{-1}(\hat{c} \circ \hat{\mathbf{e}})$   
13: **if**  $\|\mathbf{z}\|_\infty \geq \gamma_1 - \beta$  or  $\|\mathbf{r}_0\|_\infty \geq \gamma_2 - \beta$  **then**  $(\mathbf{z}, \mathbf{h}) := \perp$   
14: **else**  
15:  $\mathbf{h} := \text{MakeHint}_q(-c\mathbf{t}_0, \mathbf{w} - c\mathbf{e} + c\mathbf{t}_0, 2\gamma_2)$   $\triangleright$  Compute  $c\mathbf{t}_0$  as  $\text{NTT}^{-1}(\hat{c} \circ \hat{\mathbf{t}}_0)$   
16: **if**  $\|\mathbf{ct}_0\|_\infty \geq \gamma_2$  or  $\text{NumberOfOne}(\mathbf{h}) > \omega$  **then**  $(\mathbf{z}, \mathbf{h}) := \perp$   
17:  $\kappa := \kappa + \ell$   
18: **return**  $\sigma = (\tilde{c}, \mathbf{z}, \mathbf{h})$

---



---

**Algorithm 3** Dilithium.Verify( $pk, M, \sigma = (\tilde{c}, \mathbf{z}, \mathbf{h})$ )

---

**Input:** Public key  $pk = (\rho, \mathbf{t}_1)$ , Message  $M \in \{0, 1\}^*$ , Signature  $\sigma = (\tilde{c}, \mathbf{z}, \mathbf{h})$   
**Output:** Result  $r \in \{0, 1\}$   
1:  $\mathbf{A} \in \mathcal{R}_q^{k \times \ell} := \text{ExpandA}(\rho)$   $\triangleright$   $\mathbf{A}$  is generated and stored in NTT Representation as  $\hat{\mathbf{A}}$   
2:  $\mu \in \{0, 1\}^{512} := H(H(\rho \parallel \mathbf{t}_1) \parallel M)$   
3:  $c := \text{SampleInBall}(\tilde{c})$   
4:  $\mathbf{w}'_1 := \text{UseHint}_q(\mathbf{h}, \mathbf{A}\mathbf{z} - c\mathbf{t}_1 \cdot 2^d, 2\gamma_2)$   $\triangleright$  Compute as  $\text{NTT}^{-1}(\hat{\mathbf{A}} \circ \text{NTT}(\mathbf{z}) - \text{NTT}(c) \circ \text{NTT}(\mathbf{t}_1 \cdot 2^d))$   
5: **return**  $\tilde{c} = H(\mu \parallel \mathbf{w}'_1)$  **and**  $\|\mathbf{z}\|_\infty < \gamma_1 - \beta$  **and**  $\text{NumberOfOne}(\mathbf{h}) \leq \omega$

---

### D. Number Theoretical Transform in Dilithium

Polynomial multiplications are one of the most expensive parts in massive lattice-based cryptographic schemes. The commonly used technique to accelerate computation is the number theoretic transform (NTT). In Dilithium, the modulus  $q$  is chosen so that  $q \equiv 1 \pmod{2n}$  and thus there exists a primitive  $2n$ -th root of unity in  $\mathbb{Z}_q$ . Concretely, the recommended parameter setting is  $q = 8380417$ ,  $n = 256$  for the sake of security, and the expected primitive 512-th root of unity is  $r = 1753$ . The NTT algorithm maps  $\mathbf{f} = f_0 + f_1x + \dots + f_{255}x^{255} \in \mathbb{Z}_q[x]/(x^{256} + 1)$  to

$$\begin{aligned} &(\mathbf{f} \bmod \mathbb{Z}_q/(x^{128} - r^{128}), \mathbf{f} \bmod \mathbb{Z}_q/(x^{128} + r^{128})) \\ &= ((f_0 + r^{128}f_{128}) + \dots + (f_{127} + r^{128}f_{255})x^{127}, \\ &\quad (f_0 - r^{128}f_{128}) + \dots + (f_{127} - r^{128}f_{255})x^{127}) \\ &\in \mathbb{Z}_q[x]/(x^{128} - r^{128}) \times \mathbb{Z}_q[x]/(x^{128} + r^{128}) \end{aligned}$$

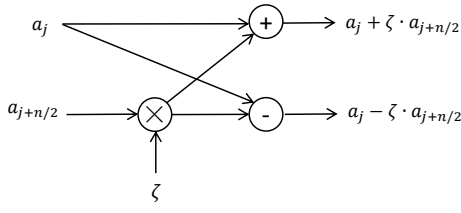
using FFT trick [32]. We call this transformation forward NTT (denoted as  $\text{NTT}$  from here on). To transform back from the NTT domain to the regular domain, the inverse NTT (denoted as  $\text{NTT}^{-1}$ ) is computed. By recursively applying this,  $\mathbf{f}$  is transformed into its NTT form

$$\begin{aligned} \text{NTT}(\mathbf{f}) = \hat{\mathbf{f}} &= (\hat{f}_0, \dots, \hat{f}_{255}) \in \mathbb{Z}_q^{256} \\ \text{where } \hat{f}_i &= \mathbf{f} \bmod (x - r^{2i-1}) = f(r^{2i-1}), i = 1, \dots, 255 \end{aligned}$$

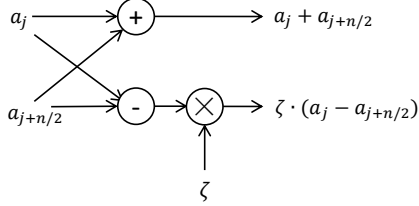
Since the NTT transform is an isomorphism, we have

$$\mathbf{f} \circ \mathbf{g} = \text{NTT}^{-1}(\text{NTT}(\mathbf{f}) \circ \text{NTT}(\mathbf{g}))$$

Note that the direct output of  $\text{NTT}/\text{NTT}^{-1}$  may not result in the natural order as presented, but in a “bit-reversed” order. However, each polynomial undergoes two times of bit reversal during NTT multiplication, one in  $\text{NTT}$  and one in  $\text{NTT}^{-1}$ , so the result finally turns out in the expected natural order. The core operation to split polynomial  $\mathbb{Z}_q[x]/(x^{256} + 1)$  to polynomial  $\mathbb{Z}_q[x]/(x^{128} - r^{128})$  and  $\mathbb{Z}_q[x]/(x^{128} + r^{128})$  is Cooley-Tukey(CT) butterfly [33]. The NTT performs 128 CT butterflies to pairs of coefficients in every iteration of splitting. Each iteration is referred to as a level. Figure 1(a) depicts the CT butterfly. One might invert the FFT trick using Gentleman-Sande(GS) butterfly [34]. Figure 1(b) depicts the GS butterfly.



(a) Cooley-Tukey butterfly



(b) Gentleman-Sande butterfly

**Fig. 1:** Butterfly diagrams

**Algorithm 4** A parallel index-based polynomial multiplication algorithm with translations

---

**Input:**  $(c, \mathbf{a})$ , where  $\mathbf{a} = [a^{(0)}, \dots, a^{(r-1)}]^T \in \mathcal{R}_q^r$ , every  $a^{(j)} = \sum_{i=0}^{n-1} a_i^{(j)} \cdot x^i \in \mathcal{R}_q$ , and  $c = \sum_{i=0}^{n-1} c_i \cdot x^i \in B_\tau$   
**Output:**  $\mathbf{u} = c \cdot \mathbf{a} = [u^{(0)}, \dots, u^{(r-1)}]^T \in \mathcal{R}_q^r$ , where  $u^{(j)} = c \cdot a^{(j)} = \sum_{i=0}^{n-1} u_i^{(j)} \cdot x^i \in \mathcal{R}_q$

---

```

1: for  $i \in \{0, 1, \dots, n-1\}$  do
2:    $w_i := 0$ 
3:    $v_i := 0$ 
4:    $v_{i-n} := 0$ 
5:   for  $j \in \{0, 1, \dots, r-1\}$  do
6:      $v_i := v_i \cdot M + (U + a_i^{(j)})$ 
7:      $v_{i-n} := v_{i-n} \cdot M + (U - a_i^{(j)})$ 
8:  $\gamma := 2U \cdot \frac{M^r - 1}{M - 1}$ 
9: for  $i \in \{0, 1, \dots, n-1\}$  do
10:  if  $c_i = 1$  then
11:    for  $j \in \{0, 1, \dots, n-1\}$  do
12:       $w_j := w_j + v_{j-i}$ 
13:  if  $c_i = -1$  then
14:    for  $j \in \{0, 1, \dots, n-1\}$  do
15:       $w_j := w_j + (\gamma - v_{j-i})$ 
16: for  $i \in \{0, 1, \dots, n-1\}$  do
17:    $t := w_i$ 
18:   for  $j \in \{0, 1, \dots, r-1\}$  do
19:      $u_i^{(r-1-j)} := (t \bmod M) - \tau U \pmod{q}$ 
20:    $t := \lfloor t/M \rfloor$ 
21: return  $\mathbf{u} = [u^{(0)}, \dots, u^{(r-1)}]^T$ 

```

---

### E. Parallel Small Polynomial Multiplication

As we shall see previously in Section II-B, one distinctive feature of the polynomial multiplication operations in Dilithium is that many of the time, one of the two multiplicands involved, namely  $c \in B_\tau$ , has exactly  $\tau$  coefficients from 1, -1, the rest being 0. Multiplication by 1 or -1 can be reduced to an addition or subtraction with a sign-based conditional judgment. This is an optimized work presented in [19]. Algorithm 4 is the parallel small polynomial multipli-

cation (PSPM) algorithm, and one single call can compute several products of  $c$  and small polynomials, it can speed up the signing and verification of Dilithium. We call lines 1-7 of pseudocode in Algorithm 4 *preparing process*, lines 9-21 *evaluating process*.

### F. AVX-512 Instructions Set

Intel Advanced Vector Extensions 512 (AVX-512) is the set of Intel's latest x64 vector instructions. AVX-512 adopts the SIMD vectorization parallel approach. Unlike the previous AVX2 instruction set, the size of the vector register is first expanded to 512 bits, and the number of vector registers is also increased from the previous 16 to 32 vector registers (zmm0–zmm31). The AVX-512 vector registers can store more values, and reduce the number of loads from memory to vector registers. In particular, there are eight mask registers in AVX-512 (k0–k7). The mask registers can be used to store the comparison results of two vector registers, enabling more comparison instructions in AVX-512. The mask register can be used for “maskmov” type instructions for masking load and store. Generally, we use this type of instructions to select the vector data lane within zmm registers we need to load or store. AVX-512 has many permutation instructions for adjusting the position of 16-bit, 32-bit, and 64-bit words residing in a zmm register. Such instructions are very important for implementing rejection sampling, NTT and NTT<sup>-1</sup>, as we shall see. AVX-512F is a vector extension of the x86 instruction set architecture (ISA) that provides 512-bit vector operations, allowing the execution of up to 16 double-precision floating-point or 32 single-precision floating-point operations per cycle. AVX-512F also includes new instructions for integer operations, gather and scatter instructions, and support for masked operations, which allows operations to be selectively applied to vector elements. AVX-512IFMA is an extension to AVX-512F that provides instructions for integer multiplication using the Fused Multiply-Add (FMA) technique, which can perform two multiply-add operations in a single instruction. AVX-512IFMA provides two new IFMA instructions for 52-bit integer vpmadd52luq and vpmadd52huq.

### III. PSPM WITH TAILORED EARLY EVALUATION (PSPM-TEE)

The signing procedure employs conditional checks for the infinity norm  $\mathbf{z}$ ,  $\mathbf{r}_0$ , and  $c\mathbf{t}_0$  to perform rejection sampling. Since these checks are performed over single coefficients, it is not necessary to compute all the polynomials of the vector. Instead, one polynomial is computed and checked immediately. If the check fails, further computation is unnecessary, saving significant computation time. The probability that  $\|\mathbf{z}\|_\infty < \gamma_1 - \beta$  is  $\left(\frac{2(\gamma_1 - \beta) - 1}{2\gamma_1 - 1}\right)^{256 \cdot \ell} = \left(1 - \frac{\beta}{\gamma_1 - 1/2}\right)^{\ell n} \approx e^{-256 \cdot \beta \ell / \gamma_1}$ , and the probability of  $\mathbf{r}_0$  in the good range is  $\left(\frac{2(\gamma_2 - \beta) - 1}{2\gamma_2}\right)^{256 \cdot k} \approx e^{-256 \cdot \beta k / \gamma_2}$ . It is worth noting that the majority of loop repetitions occur due to the infinity checks of  $\mathbf{z}$  and  $\mathbf{r}_0$ . Therefore, we will only consider the probabilities of these two vectors. In previous implementations, the infinite norm of the vector  $\mathbf{z}$  was first evaluated, followed by the

evaluation of the infinite norm of vector  $\mathbf{r}_0$ . In this paper, for the first time, we propose to adjust the order of evaluation of vector  $\mathbf{z}$  and vector  $\mathbf{r}_0$  based on the different rejection probabilities of vector  $\mathbf{z}$  and vector  $\mathbf{r}_0$  for different parameters of Dilithium. We can compute the probabilities of the two conditional checks for three parameter sets. As shown in Table I, the probability of vector  $\mathbf{z}$  falling within a good range is always greater than the probability of vector  $\mathbf{r}_0$ . Hence, checking  $\mathbf{r}_0$  prior to checking  $\mathbf{z}$  can result in a faster signature procedure since repetition is more likely to occur after checking  $\mathbf{r}_0$  and the computation of  $\mathbf{z}$  can be saved. We tested the performance of the Dilithium C REF implementation between checking  $\mathbf{r}_0$  first and checking  $\mathbf{z}$  first. We observe that checking  $\mathbf{r}_0$  before checking  $\mathbf{z}$  results in a 2% to 3% improvement in the signing procedure, as demonstrated in Table II. The idea of first evaluating the infinite norm of the vector with higher rejection probability is applicable to signature schemes that use rejection sampling.

The parallel algorithm presented in [19] poses difficulties for *early-evaluation* as it calculates the entire polynomial vector multiplication results simultaneously. To overcome this issue, we introduce a PSPM algorithm in this section that incorporates early evaluation. Our algorithm includes the computation of  $c \cdot \mathbf{s} + \mathbf{y}$  and  $\text{LowBits}(\mathbf{w} - c \cdot \mathbf{e}, 2\gamma_2)$  in the evaluating process, enabling us to promptly perform reject checks for each coefficient. If the reject checks fail, the computation is terminated. This approach results in faster signature speeds. Additionally, there are various PSPM algorithms available. In Dilithium3/5, the coefficients of  $\mathbf{s}$  and vector  $\mathbf{e}$  are stored in separate precomputed tables, allowing for independent early checks of  $\mathbf{z}$  and  $\mathbf{r}_0$ . In contrast, Dilithium2 stores the coefficients of  $\mathbf{s}$  and  $\mathbf{e}$  in the same precomputed table. Consequently, the early checks for  $\mathbf{z}$  and  $\mathbf{r}_0$  are performed simultaneously, as depicted in Algorithm 5. It is important to note that during rejection checks, verifying the  $\mathbf{r}_0$  always takes precedence over checking vector  $\mathbf{z}$  for all three parameter sets of Dilithium, as previously analyzed.

Scheme	$\Pr(\ \mathbf{z}\  \leq \gamma_1 - \beta)$	$\Pr(\ \mathbf{r}_0\  \leq \gamma_1 - \beta)$
Dilithium2	0.543591	0.429801
Dilithium3	0.619647	0.315712
Dilithium5	0.663515	0.389636

TABLE I: Probability of vector in a good range.

Scheme	Round3 C REF		Imp. (%)
	(check $\mathbf{z}$ first)	(check $\mathbf{r}_0$ first)	
Dilithium2	992696	972244	2.06%
Dilithium3	1670374	1627560	2.56%
Dilithium5	2088720	2026818	2.96%

TABLE II: Comparative performance of checking  $\mathbf{z}$  first and checking  $\mathbf{r}_0$  first (Cycles).

Scheme	Sign (Original PSPM)	Sign (Improved PSPM)	Imp.(%)
Dilithium2	670970	636326	5.16%
Dilithium3	1171086	1101330	6.00%
Dilithium5	1491124	1415452	5.07%

TABLE III: Comparative performance of improved PSPM and original PSPM [19] (Cycles).

Algorithm 5 A parallel index-based polynomial multiplication algorithm with early evaluating  $\mathbf{r}_0$  and  $\mathbf{z}$  for Dilithium2

**Input:**  $(c, \mathbf{s}, \mathbf{e}, \mathbf{y}, \mathbf{w})$ , where  $\mathbf{s} = [s^{(0)}, \dots, s^{(l-1)}]^T \in \mathcal{R}_q^l, \mathbf{y} \in \mathcal{R}_q^l, \mathbf{e} \in \mathcal{R}_q^k, \mathbf{w} \in \mathcal{R}_q^k$ , every  $s^{(j)} = \sum_{i=0}^{n-1} s_i^{(j)} \cdot x^i \in \mathcal{R}_q, y^{(j)} = \sum_{i=0}^{n-1} y_i^{(j)} \cdot y^i \in \mathcal{R}_q, e^{(j)} = \sum_{i=0}^{n-1} e_i^{(j)} \cdot e^i \in \mathcal{R}_q, w^{(j)} = \sum_{i=0}^{n-1} w_i^{(j)} \cdot w^i \in \mathcal{R}_q$ , and  $c = \sum_{i=0}^{n-1} c_i \cdot x^i \in B_\tau$   
**Output:**  $\mathbf{z} = c \cdot \mathbf{s} + \mathbf{y} = [z^{(0)}, \dots, z^{(l-1)}]^T \in \mathcal{R}_q^l$ , where  $z^{(j)} = c \cdot s^{(j)} + y^{(j)} = \sum_{i=0}^{n-1} z_i^{(j)} \cdot x^i \in \mathcal{R}_q, \mathbf{r} = \mathbf{w} - c \cdot \mathbf{e} = [r^{(0)}, \dots, r^{(k-1)}]^T \in \mathcal{R}_q^k$ , where  $r^{(j)} = w^{(j)} - c \cdot e^{(j)} = \sum_{i=0}^{n-1} r_i^{(j)} \cdot x^i \in \mathcal{R}_q$   
1: **for**  $i \in \{0, 1, \dots, n-1\}$  **do**  
2:    $m_i := 0$   
3:    $v_i := 0$   
4:    $v_{i-n} := 0$   
5:   **for**  $j \in (0, 1, \dots, l-1)$  **do**  
6:      $v_i := v_i \cdot M + (U + s_i^{(j)})$   
7:      $v_{i-n} := v_{i-n} \cdot M + (U - s_i^{(j)})$   
8:   **for**  $j \in (0, 1, \dots, k-1)$  **do**  
9:      $v_i := v_i \cdot M + (U + e_i^{(j)})$   
10:      $v_{i-n} := v_{i-n} \cdot M + (U - e_i^{(j)})$   
11:  $\gamma := 2U \cdot \frac{M^{l+k-1}}{M-1}$   
12: **for**  $i \in \{0, 1, \dots, n-1\}$  **do**  
13:   **if**  $c_i = 1$  **then**  
14:     **for**  $j \in \{0, 1, \dots, n-1\}$  **do**  
15:        $m_j := m_j + v_{j-i}$   
16:   **if**  $c_i = -1$  **then**  
17:     **for**  $j \in \{0, 1, \dots, n-1\}$  **do**  
18:        $m_j := m_j + (\gamma - v_{j-i})$   
19: **for**  $i \in \{0, 1, \dots, n-1\}$  **do**  
20:    $t := m_i$   
21:   **for**  $j \in (0, 1, \dots, k-1)$  **do**  
22:      $r_i^{(k-1-j)} := (t \bmod M) - \tau U \pmod{q}$   
23:      $r_i^{(k-1-j)} := w_i^{(k-1-j)} - r_i^{(k-1-j)}$   
24:      $r_i^{(k-1-j)} := \text{LowBits}_q(r_i^{(k-1-j)}, 2\gamma_2)$   
25:     **if**  $|r_i^{(k-1-j)}| \geq \gamma_2 - \beta$  **then** Restart signature process.  
26:      $t := \lfloor t/M \rfloor$   
27:   **for**  $j \in (0, 1, \dots, l-1)$  **do**  
28:      $z_i^{(l-1-j)} := (t \bmod M) - \tau U \pmod{q}$   
29:      $z_i^{(l-1-j)} := z_i^{(l-1-j)} + y_i^{(l-1-j)}$   
30:     **if**  $|z_i^{(l-1-j)}| \geq \gamma_1 - \beta$  **then** Restart signature process.  
31:      $t := \lfloor t/M \rfloor$   
32: **return**  $\mathbf{z} = [z^{(0)}, \dots, z^{(l-1)}]^T, \mathbf{r} = [r^{(0)}, \dots, r^{(k-1)}]^T$

#### IV. TAILORED REDUCTION

We present an optimized modular reduction tailored for Dilithium modulus  $q = 8380417$ , which might be of independent interest and can be applied to optimize the implementations of Dilithium in other platforms. The modulus  $q$  can be represented as  $2^{23} - 2^{13} + 1$ . We can apply a fast specialized reduction algorithm for modulus prime having such a form.

We exemplify with the Dilithium prime and the process is shown in Algorithm 6.

**Algorithm 6** Tailored reduction for the Dilithium prime  $q = 2^{23} - 2^{13} + 1$

**Require:**  $-2^{40} < z \leq 2^{40}, q = 2^{23} - 2^{13} + 1$

**Ensure:**  $r = z \pmod{q}, -2^{31} < r < 2^{31}$

- 1:  $p_1 = \lfloor \frac{z}{2^{23}} \rfloor$
- 2:  $r = z - qp_1$

**Proposition 1.** If  $-2^{40} < z \leq 2^{40}$ , then Algorithm 6 computes an integer  $r$  congruent to  $z$  modulo  $q = 2^{23} - 2^{13} + 1$  such that  $-2^{31} < r \leq 2^{31}$ .

*Proof.* If  $-2^{40} < z \leq 2^{40}$ , in line 1,  $p_1 = \lfloor z/2^{23} \rfloor < 2^{17}$ , let  $r_1 = z - 2^{23}p_1 < 2^{23}$ ,  $r = z - qp_1 = z - (2^{23} - 2^{13} + 1)p_1 = (2^{13} - 1)p_1 + r_1$ , so

$$|r| \leq |(2^{13} - 1)p_1| + |r_1| \leq (2^{13} - 1)2^{17} + 2^{23} < 2^{31}.$$

□

**Algorithm 7** Signed Montgomery reduction for 32-bit  $q$  [32]

**Require:**  $0 < q < 2^{31}$  odd,  $-2^{31}q \leq z = z_12^{32} + z_0 < 2^{31}q$  where  $0 \leq z_0 < 2^{32}$

**Ensure:**  $r' \equiv \beta^{-1}z \pmod{q}, -q < r' < q$

- 1:  $m \leftarrow z_0q^{-1} \pmod{\pm 2^{32}} \triangleright$  signed low product,  $q^{-1}$  precomputed
- 2:  $t_1 \leftarrow \left\lfloor \frac{mq}{\beta} \right\rfloor \triangleright$  signed high product
- 3:  $r' \leftarrow z_1 - t_1$

## A. Comparisons

Montgomery reduction is an efficient algorithm to reduce product in NTT by computing Hensel remainder. The disadvantage of Montgomery reduction is the Hensel remainder  $r'$  is congruent to  $z \cdot 2^{-32} \pmod{q}$  instead of representative of the residue class of  $z$  modulo  $q$ . Algorithm 7 presents the pseudocode of Signed Montgomery reduction. This operation involves two bit-shiftings, two multiplications, and one subtraction. In contrast, our Tailored reduction algorithm is more efficient as it only requires one bit-shifting, one subtraction, and one multiplication. This makes it a better choice than Montgomery reduction when dealing with products smaller than  $2^{40}$  for NTT with lazy reduction. Furthermore, the Tailored reduction can be implemented with the new AVX-512IFMA instruction in just two instructions, resulting in a lower latency during reduction (see Subsection V-C for a detailed discussion).

## V. IMPLEMENTATION DETAILS

We present an optimized vectorization implementation of Dilithium for CPUs that both support the AVX2 and AVX-512 instruction sets. In this section, we will thoroughly explore the implementation details of each optimized module.

**TABLE IV:** Percentages of used functions in Keygen, Signature and Verification.

Functions	Keygen	Sign	Verify
montgomery_reduce	38.24%	23.02%	16.04%
KeccakF1600_StatePermute	17.68%	38.84%	42.99%
invntt_tomont	17.48%	6.28%	5.22%
ntt	6.94%	9.30%	3.35%
poly_pointwise_montgomery	4.96%	1.86%	2.22%

## A. Dilithium Software Performance Profiling

A critical step in software optimization is to identify the performance bottlenecks of the algorithm. In this section, we utilize the Linux performance analysis tool perf to profile the Dilithium C REF implementation of Dilithium3 parameter set. The performance data was collected by executing the Dilithium3 codes 1000 times and calculating the average execution time. Table IV depicts the detailed percentages. KeccakF1600\_StatePermute which is predominantly used in hash functions, is the most time-consuming function in key generation, signing, and verification. This is followed by Montgomery reduction and poly\_uniform and poly\_uniform\_eta, and then NTT and NTT<sup>-1</sup>. The functions of poly\_uniform and poly\_uniform\_eta are used to sample coefficients using the rejection sampling method, while the functions of NTT, NTT<sup>-1</sup> and Montgomery reduction are used for polynomial multiplication. Consequently, we can identify the computation bottleneck functions as polynomial multiplication, hash function, and rejection sampling. In the following sections, we propose a series of optimization techniques for these functions.

## B. Data Alignment

We represent each polynomial as an array of 256 32-bit signed integers. For this representation, we can use the AVX-512 SIMD instruction to vectorize different functions. Alternatively, we can represent this array as an array of 16 512-bit vectors of type \_\_m512i in AVX-512 intrinsics, where the symbol “i” represents integers. In AVX-512 assembly, we store the 256 coefficients in 16 zmm vector registers. The 512-bit Intel AVX-512 registers have an alignment requirement of 64 bytes to ensure optimal vectorization. Optimal memory access is achieved when the data starts at an address on a 64-byte boundary, which means that the address in memory is divisible by 64. Therefore, we align all arrays to 64 bytes in our implementation.

## C. Vectorization of NTT with AVX-512

We now give details about our AVX-512 parallel implementation of NTT for Dilithium polynomial ring  $\mathbb{Z}_q[x]/(x^n + 1)$ , where  $n = 256$ ,  $q = 8380417$ , the modulus  $q$  is a 32-bit prime. The whole NTT-based polynomial multiplication is divided into three parts, NTT, NTT<sup>-1</sup>, and point-wise multiplication.

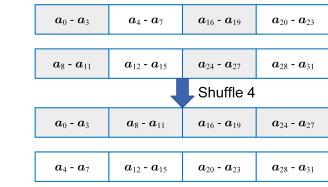
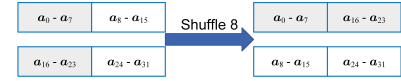
a) *Register allocation:* Here we introduce our register arrangement. Note that AVX-512 has 32 512-bit vector zmm registers (zmm0-zmm31). If a 32-bit integer is directly stored in a zmm vector register without zero-padded, a zmm register can store 16 32-bit coefficients, and hence 16 vector registers are enough to load all 256 coefficients. In doing so, we merge the eight levels without reloading coefficients. Later in the implementation of the butterfly implementation, we will carefully explain why there is no need to reserve 64-bit space for intermediate products. We arrange zmm1-zmm16 to store all the polynomial coefficients consecutively. We use zmm17 to store the precomputed results  $\zeta q^{-1} \bmod 2^{32}$ , and zmm18 to store  $\zeta$  ( $\zeta$  is the twiddle factor). The zmm19, zmm20, and zmm21 are used to store temporary computation values.

	low	—	high		low	—	high		low	—	high		low	—	high
zmm1	$a_0$	—	$a_{15}$	zmm5	$a_{64}$	—	$a_{79}$	zmm9	$a_{128}$	—	$a_{143}$	zmm13	$a_{192}$	—	$a_{207}$
zmm2	$a_{16}$	—	$a_{31}$	zmm6	$a_{80}$	—	$a_{95}$	zmm10	$a_{144}$	—	$a_{159}$	zmm14	$a_{208}$	—	$a_{223}$
zmm3	$a_{32}$	—	$a_{47}$	zmm7	$a_{96}$	—	$a_{111}$	zmm11	$a_{160}$	—	$a_{175}$	zmm15	$a_{224}$	—	$a_{239}$
zmm4	$a_{48}$	—	$a_{63}$	zmm8	$a_{112}$	—	$a_{127}$	zmm12	$a_{176}$	—	$a_{191}$	zmm16	$a_{240}$	—	$a_{255}$

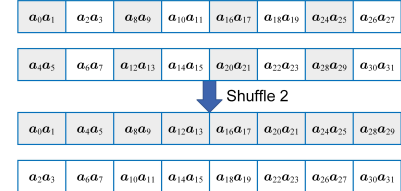
Fig. 2: The storage coefficients order in zmm registers

b) *Coefficients loading and shuffling:* We exemplify a polynomial  $a_0 + a_1x + \dots + a_{255}x^{255}$  as input of NTT. Before the first level, we load the consecutive 16 coefficients in every zmm register as shown in Figure 2. In the first level, the distance of CT butterfly is 128. So the two vector registers zmm1 and zmm9 perform a pair of butterfly operations, and zmm2 and zmm10 perform a pair of butterfly operations; that is, the subscript distance of zmm register is 8. In the second level, the distance is 64. The corresponding registers subscript distance becomes 4. Analogously, the registers subscript distances in the third level and fourth level are two and one respectively. Starting from the fifth level, the distance is 8 while a consecutive 16 coefficients reside in a zmm register. Therefore, in the fifth level, we need to swap the upper 8 coefficients of one register with the lower 8 coefficients of another register. After the fifth level, coefficients are stored in a permuted order in registers. In the sixth level, the distance is 4. The upper four coefficients and the lower four coefficients in every 256-bit data lane are shuffled. Similarly, two coefficients are swapped in every 128-bit data lane in the seventh level and one coefficient is shuffled in every 64-bit data lane in the eighth level. The shuffling process is illustrated in Figure 3(a), Figure 3(b), and Figure 3(c). Shuffle8 means to shuffle 8 coefficients, Shuffle4 means to shuffle 4 coefficients, Shuffle2 means to shuffle 2 coefficients, and Shuffle1 means to shuffle one coefficient. We implement Shuffle8 using the vshufi32x4 instruction. The function of this instruction is to rearrange each 128-bit data lane of the two vector registers a and b through an 8-bit immediate value. We want to rearrange eight consecutive coefficients, which correspond to a 128-bit data lane. According to the instruction pseudocode<sup>1</sup>, we set the immediate value to 0x44 and 0xEE.

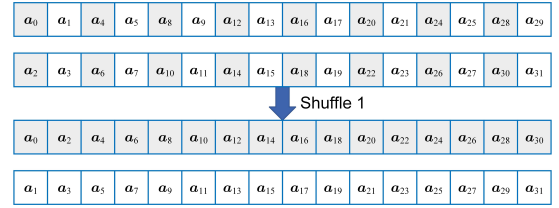
The shuffling of the four coefficients is more complicated because at this time the four consecutive coefficients



(a) shuffle eight and four coefficients



(b) shuffle two coefficients



(c) shuffle one coefficients

Fig. 3: Coefficients shuffling in two vector registers

correspond to a 64-bit data lane. Here we use two permute instructions, one is vpermq and the other is vpblendmd. First, we splice the lower 64-bit in register a and the lower 64-bit in register b using vpblendmd. However, this instruction can only be spliced by the value of the mask register according to the index. Specifically, if we use the vpblendmd directly, the order of the coefficients we will obtain is  $\{a_0, a_1, a_2, a_3, b_4, b_5, b_6, b_7, a_8, a_9, a_{10}, a_{11}, b_{12}, b_{13}, b_{14}, b_{15}\}$ . This is not the order we want. Therefore, we duplicate the lower 64 bits to the upper 64 bits of register b in every 128-bit data lane and duplicate the upper 64 bits to the lower 64 bits of register a in every 128-bit data lane. We implement this by using vpermq with constant argument 0x4E and then using the vpblendmd instruction to splice the 64-bit data lane in the two registers through the mask register. Here, we use the kmovw instruction to store 0x0F0F into mask register k6. For the permutation of two coefficients, we use vpunpcklqdq and vpunpckhqdq. For the shuffling of one coefficient, because there is no ready-made instruction that can be realized, we adopt the same idea as shuffling four coefficients. First, the upper 32 bits of every 64 bits data lane in register b are obtained by shifting 32 bits to the left. Then use the vpblendmd to splice 32 bits of the two registers with mask register value 0xAAAA. For copying the upper 32-bit to the lower 32-bit, we directly use the vmovshdup to copy the upper 32-bit.

c) *Butterflies:* In Section II-D, we introduce NTT and CT/GS butterflies. In the CT butterfly transform, half of the

<sup>1</sup><https://www.intel.com/content/www/us/en/docs/intrinsics-guide/index.html>

coefficients need to be multiplied by the twiddle factors. Note that the twiddle factors are fixed constants, so we precompute their values and store them in a look-up table. As mentioned earlier, to save multiplication in Montgomery reduction, we also precompute  $\zeta q^{-1} \bmod 2^{32}$  and store them in the look-up table. Here we would like to explain why it is not necessary to reserve 64-bit for multiplication results. At the start, the 16 consecutive coefficients are loaded into a `zmm` register. During the butterfly operation calculation, we split the coefficients that need to be multiplied by the twiddle factor into two parts according to the odd and even subscripts. The odd and even subscript coefficients are stored in two `zmm` registers. The odd/even coefficient splitting is achieved by copying the upper 32 bits using `vmovshdup` instruction. After splitting, a register only stores eight coefficients, and each coefficient occupies 64 bits of space. Thus, there is no need to reserve 64 bits of space when loading. Finally, it is reduced to 32-bit by Montgomery reduction. Then the odd-index and even-index coefficients are spliced into a 512-bit vector register by `vpblendmd` instruction. In this way, although the splitting operation takes some clock cycles, it ensures the maximum degree of parallelism. Generally speaking, this implementation idea is faster than the idea of loading zero-padded 64-bit integers.

---

**Algorithm 8** 2-instruction Tailored reduction using AVX512IFMA

---

**Input:** A 40-bit signed integer  $2^{-40} < z \leq 2^{40}$   
**Output:**  $r = z(\bmod q)$ ,  $-2^{31} < r < 2^{31}$

```

1: vpsrlq 23,  $z, r$   $\triangleright \frac{z}{2^{23}}$ 
2: vpmadd52luq  $-q, z, r$   $\triangleright z - \frac{z}{2^{23}} \cdot q$ 
3: return  $r$ 
```

---



---

**Algorithm 9** 3-instruction Tailored reduction using AVX512

---

**Input:** A 40-bit signed integer  $2^{-40} < z \leq 2^{40}$   
**Output:**  $r = z(\bmod q)$ ,  $-2^{31} < r < 2^{31}$

```

1: vpsrlq 23,  $z, r$   $\triangleright \frac{z}{2^{23}}$ 
2: vpmuldq  $q, z, t$   $\triangleright t = \frac{z}{2^{23}} \cdot q$ 
3: vpsubq  $t, z, r$   $\triangleright r = z - t$ 
4: return  $r$ 
```

---

*d) Vectorized Tailored reduction:* We present a vectorized Tailored reduction implementation using AVX-512IFMA instruction. We use this vectorized Tailored reduction implementation in  $\text{NTT}(\mathbf{t}_0)$  and  $\text{NTT}(\mathbf{t}_1)$ . Previous work implements a four-instruction Montgomery reduction that is both suited for AVX2 and AVX-512 vectorized implementation. The total latency of these four instructions is 12 cycles. In this work, we present a 2-instruction Tailored reduction using AVX-512IFMA `vpmadd52luq` instruction that can reduce both latency and instruction count and shown in Algorithm 8. This vectorized Tailored reduction reduces the cycle counts down to 6 cycles by eliminating one `vpmuldq` and one `vpsubq`.

---

**Algorithm 10** 4-instruction Montgomery reduction using AVX512 [13]

---

**Input:** A signed integer  $2^{-31}q < z \leq 2^{31}q$   
**Output:**  $r' = 2^{-32}z(\bmod q)$ ,  $-q < r' < q$

```

1: vpmuldq  $q^{-1}, z, m$   $\triangleright m = z \bmod 2^{32} \cdot q^{-1}$ 
2: vpmuldq  $q, m, t$   $\triangleright t = m \bmod 2^{32} \cdot q$ 
3: vpsubq  $t, z, r'$   $\triangleright r' = z - t$ 
4: vpsrlq 32,  $r', r'$   $\triangleright r' = \frac{r'}{2^{32}}$ 
5: return  $r'$ 
```

---

*e) Lazy reduction:* Dilithium involves NTT operations on polynomials with small coefficients. We observe that, for CT butterfly of NTT with small coefficients such as  $c$  and the noise vectors  $\mathbf{s}$  and  $\mathbf{e}$ , the first level does not need to perform Montgomery reduction, because the upper bound data width of  $\mathbf{s}/\mathbf{e}$  is 4 bits, and the multiplication of a 4-bit coefficient and a 23-bit twiddle factor will not exceed 32 bits.  $c$  is a small polynomial with only  $\tau \pm 1$ , so the product of a 1-bit coefficient and a 23-bit twiddle factor will not exceed 32 bits as well. Specifically, we do not need to perform modular reductions in the first level of  $\text{NTT}(c)$ ,  $\text{NTT}(\mathbf{s})$  and  $\text{NTT}(\mathbf{e})$ . For  $\text{NTT}(\mathbf{t}_0)$  and  $\text{NTT}(\mathbf{t}_1)$  in all the three security levels of Dilithium2/3/5, as well as  $\text{NTT}(\mathbf{y})$  in Dilithium2, in the first level of NTT we only need to perform the above tailored reduction algorithm instead of Montgomery reduction. For instance, in Dilithium2, where  $\gamma_1 = 2^{17}$ , the data width of vector  $\mathbf{y}$  is 18-bit. The product of vector  $\mathbf{y}$  and the twiddle factor multiplication is a 41-bit integer in  $(-2^{40}, 2^{40}]$ . Hence, we use the Tailored reduction Algorithm 6 proposed above. Specifically, in this case, we do not need to completely reduce the coefficient to  $\mathbb{Z}_q$  in the first level of NTT, our only requirement is to prevent the coefficient from overflowing. Starting from the second level, the product will be reduced by Montgomery reduction.

#### D. Hashing

Dilithium makes use of XOF to expand seeds and sample polynomials. SHAKE-128 is used to generate matrix  $\mathbf{A}$ , and SHAKE-256 is used to generate vectors  $\mathbf{s}, \mathbf{e}$  and  $\mathbf{y}$ . As we discussed in Section V-A, hashing is an expensive operation in the entire scheme. The previous AVX2 implementation used a 4-way SHAKE-128 and SHAKE-256; that is, they use a vectorized SHAKE implementation that operates on 4 parallel sponges and hence can absorb and squeeze blocks in and out of these 4 sponges at the same time [13]. We use the AVX-512 implementation and can calculate and generate 8 hash results at the same time due to the expansion of the register bit width. We used the SPHINCS+ AVX-512 open source code<sup>2</sup>. We embedded this 8-way hash implementation into the expansion of matrix  $\mathbf{A}$ , vector  $\mathbf{y}$ , and vector  $\mathbf{s}, \mathbf{e}$ .

#### E. Parallel Rejection Sampling

The rejection sampling process generates a 23-bit random number by sampling and then checks whether it is greater than or less than  $q$  using conditional judgment. If the number is greater than  $q$ , it is rejected, and if it is less than  $q$ , it

<sup>2</sup><https://github.com/DorAlter/sphincsplus/tree/avx512-implementation>



is accepted. To obtain the 23-bit random number, the byte stream obtained by hashing needs to be spliced, and then the random number is accepted or rejected sequentially. This process poses a challenge to vectorizing rejection sampling. The previous method used by AVX2 was to create a two-dimensional array of size  $2^8 \times 8 = 2048$ , which stored all possible acceptance positions for 8 32-bit integers in a 256-bit vector register. However, this method is not suitable for AVX-512 implementation because a vector register in AVX-512 can store 16 32-bit integers, requiring a two-dimensional array of size  $2^{16} \times 16 = 1048576$ , which is not feasible for AVX-512 implementation. Therefore, a more space-efficient implementation method was used.

One of the main concepts of rejection sampling is to compare numbers in all positions with  $q$  and then store them in order. Fortunately, AVX-512 has a built-in function called `_mm512_mask_compressstoreu_epi32`, which stores 32-bit integers in their corresponding positions sequentially through the values of the mask register. This allows us to compressively store the values and meet our requirements. The function is described in Figure 4. We can also set the mask register using the function `_mm512_cmp_epi32_mask`. By setting the comparison operand value of the `_mm512_cmp_epi32_mask` function to `_MM_CMPINT_LT`, we compare the values of the input vector register **a** and vector register **b**. If **a** is smaller than **b**, we set the value of the mask register at the corresponding position to 1, otherwise, we set it to 0. Note that the mask register is a 16-bit binary integer. We can determine how many coefficients are received in a vector register by counting the number of 1's in the mask register using the function `_mm_popcnt_u32`.

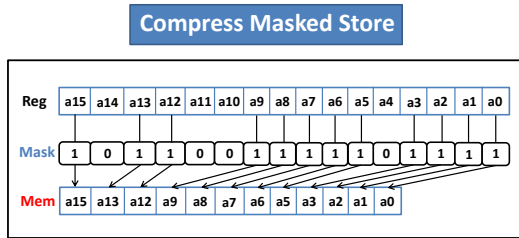
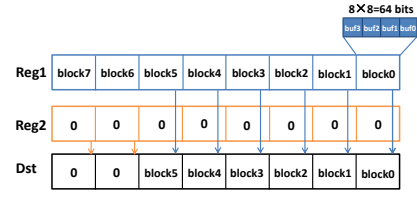


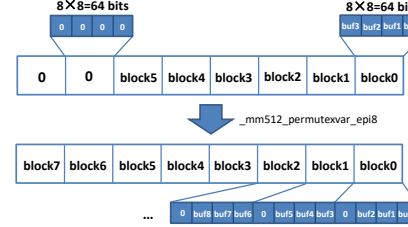
**Fig. 4:** The `_mm512_mask_compressstoreu_epi32` function.

We optimized the vectorized implementation of generating 23-bit random integers to reduce the number of calls to SHAKE-128. Since we only need 48 out of the 64 bytes streams loaded to obtain 16 23-bit numbers, we should avoid wasting the extra 16 bytes generated by SHAKE-128.

To achieve this, we first initialize a vector register with all zeros, and then use the functions `_mm512_permutexvar_epi8` and `_mm512_mask_blend_epi64` to adjust and splice this all-0 register and the register loaded with 64-byte random byte streams. We illustrate this process in Figure 5(a) and Figure 5(b). The upper  $6 \times 64 = 384$  bits are the random byte streams, and the lower  $2 \times 64 = 128$  bits are zeros. By adjusting the



(a) `_mm512_mask_blend_epi64`



(b) `_mm512_permutexvar_epi8`

**Fig. 5:** Packing random byte stream

order of the spliced vector registers in the 8-bit data lane using the function `_mm512_permutexvar_epi8`, we can obtain three consecutive random bytes of every four bytes, and the last byte of the four bytes is just 0. Then, we use `_mm512_and_si512` to perform a bitwise AND with 23 ones to obtain 16 23-bit random integers.

The above describes the rejection sampling process for generating numbers in the range  $[0, q)$ . However, in Dilithium, there is also rejection sampling of numbers in the range  $[-\eta, \eta]$ . We have also optimized the previous AVX2 implementation for this purpose. In our implementation, we first separate the high 4 bits and low 4 bits of each 8-bit random byte, and then use the `_mm512_cmp_epi32_mask` function to judge and store the high 4 bits and low 4 bits separately using mask registers. To ensure the correctness of the test vector, we also adjust the order of the high 4 bits and low 4 bits accordingly.

#### F. Expanding Matrix **A** and Sampling Vectors

We present an 8-way `poly_uniform_8x` function to sample 8 polynomials in  $R_q$  simultaneously, using 8-way SHAKE-128 and parallel rejection sampling. For the expansion of matrix **A**, in Dilithium2 where  $k = l = 4$ , we can directly call the `poly_uniform_8x` function twice to generate 4 row vectors. In Dilithium3, where  $k = 6, l = 5$ , `poly_uniform_8x` is called four times to generate 30 polynomials of 6 row vectors. In Dilithium5, `poly_uniform_8x` is called eight times to generate 56 polynomials of 8 row vectors. Similarly, for sampling vectors, we propose an 8-way function `poly_uniform_eta_8x` and `poly_uniform_gamma1_8x` using 8-way SHAKE-256 to sample vectors **s/e** and **y** respectively.

### G. Implementing PSPM-TEE

This work implements AVX2 and AVX-512 for PSPM-TEE. In original PSPM implementation from [19], coefficients were packed into 64-bit words. However, to ensure consistency in the data lane of the vector register and make it easier to operate on the same size operand, we chose to pack coefficients into 32-bit words. This eliminates the need to zero-extend 32-bit coefficients to 64-bit and simplifies the vectorization of PSPM implementation. For Dilithium2/3/5, we provide a specific description of the implementation of the parallel small polynomial algorithm for Dilithium3 parameters, where  $k = 6, l = 5$ . Our implementation is based on the parallel small polynomial parameter sets shown in Table X in Appendix A.

Firstly, we introduce the splicing of the noise vector  $\mathbf{s}, \mathbf{e}$ . Although each coefficient of  $\mathbf{s}$  and  $\mathbf{e}$  lies in the range of  $[-4, 4]$ , the coefficients grow by  $2\tau U$  after the addition operation in Algorithm 4, where  $U = 4, \tau = 49$  in Dilithium3. As a result, the upper bound of coefficients is 392. Therefore, each coefficient needs to set aside at least 9 bits for storage. One 32-bit word can pack up to 3 polynomial coefficients. Therefore, vectors  $\mathbf{s}, \mathbf{e}$  need two precomputed tables to store all coefficients.

The preparing process is implemented using intrinsic functions because it is easily vectorizable. However, the loop operation in Algorithm 4 is not suitable for parallel implementation. Therefore, our AVX-512 implementation uses parallel computing to implement the accumulation process through AVX-512 assembly. Specifically, when determining whether challenge polynomial  $c$  is 1 or -1, we pass the corresponding array address to AVX-512 assembly and perform parallel addition. Combining with the parallelism achieved by Algorithm 5, the implementation of  $\mathbf{cs}$  can achieve a maximum of  $8 \times 3 = 24$  parallelism at most.

We implemented the evaluating process of extracting computation results from the 32-bit packed words using the intrinsic functions. To perform the conditional check of vector coefficients, we used the `_mm512_cmp_epi32_mask` function, which allows us to check 8 coefficients in parallel and obtain a 16-bit mask for every 32-bit data lane. If the mask is non-zero, the function immediately returns 1.

### H. Vectorized Packing

*a) Obstacle in vectorizing packing:* In Dilithium implementation, polynomial vectors need to be encoded as byte strings (packing) and vice versa (unpacking). We have completed the vectorization of unpacking of  $\mathbf{z}$  and packing of  $\mathbf{w}_1$  using AVX-512. To ensure that our optimized implementation works on all platforms and matches the NIST Known Answer Tests (KAT) test vectors, we faced a difficulty in vectorizing polynomial packing and unpacking. Directly vectorizing the packing/unpacking process is not feasible. For instance, a 512-bit vector register can store 16 coefficients, and bit-wise instructions are operated on two vector registers. If register  $\mathbf{r}_1$  stores coefficients  $a_0 - a_{15}$ ,  $\mathbf{r}_2$  stores coefficients  $a_{16} - a_{31}$ . A pair of coefficients  $a_0$  and  $a_{16}$  are packed, whereas we need  $a_0$  and  $a_1$ . Therefore, direct vectorization is not possible.

*b) How to vectorize packing:* The vectorization of unpacking  $\mathbf{z}$  using AVX-512 is similar to parallel rejection sampling, we do not give details again here. For packing of  $\mathbf{w}_1$ . In Dilithium3 and Dilithium5, the coefficient range of  $\mathbf{w}_1$  is  $[0, 15]$ . Therefore, every two  $\mathbf{w}_1$  coefficients can be packed into one byte. A `zmm` register can store 128 4-bit  $\mathbf{w}_1$  coefficients. Therefore, 128 polynomial coefficients are loaded continuously in each loop. We use `_mm512_packus_epi32` to convert packed signed 32-bit integers to packed 16-bit integers. Next, we use `_mm512_packus_epi16` to convert packed 16-bit integers to packed 8-bit integers, which results in 64 coefficients stored in each vector, with each coefficient having a width of 8 bits. We then use `_mm512_maddubs_epi16` to shift the coefficients with odd indices by 4 bits to the left, so that adjacent coefficients are combined into one byte. Finally, we use `_mm512_maddubs_epi16` to merge all coefficients into a 512-bit vector. However, after the above operation, we change the order of the coefficients. Therefore, we use the intrinsic functions `_mm512_permutexvar_epi32` and `_mm512_shuffle_epi8` to reorder the coefficients to ensure the correctness of the KAT test.

## VI. EXPERIMENT RESULTS AND DISCUSSIONS

We implemented all three security levels of Dilithium: Dilithium2, Dilithium3, and Dilithium5, using both C language and Intel AVX-512 assembly and AVX-512 intrinsic functions. We also optimized the previous AVX2 code using the presented optimization technique. Our optimized vectorization implementation passed the NIST Known Answer Tests tests to ensure the implementation works on all platforms. We perform a detailed evaluation of performance improvements for the optimization we have achieved in Section V. The Dilithium codes are collected from <https://csrc.nist.gov/Projects/post-quantum-cryptography/selected-algorithms-2022>. The compiler is gcc-9.4.0 and the optimization flags are `-Wshadow -Wpointer-arith -mavx2 -mAVX-512F -mavx512vbmi -mavx512bw -mavx512cd -mavx512vl -mpopcnt -maes -march=native -mtune=native -O3`. The benchmark experiments were conducted on a desktop machine with Ubuntu 20.04 operating system and Intel(R) Core(TM) i7-11700F CPU (Rocket Lake) running at 2.5GHz. As usual, we disable the TurboBoost and Hyper-Threading to ensure the reproduction of the experiments. Each experiment is repeated 100000 times, and we present the median results.

### A. Tailored Reduction Performance

We implemented Tailored reduction using AVX2 and AVX-512 in the first level of NTT. We make a comparison with NTT using Montgomery reduction. To demonstrate the true benefits of Tailored reduction in the signing process, we compared the original AVX2 signing implementation with the AVX2 implementation using Tailored reduction in the  $\text{NTT}(t_0)$ . In Table V, Sign-original refers to the implementation of signing with NTT using Montgomery reduction. Sign-opt1 refers to the implementation of signing with NTT using Tailored reduction by AVX-512F. Sign-opt2 refers to the implementation of signing with NTT using Tailored reduction by AVX-512IFMA.

Table V shows that Tailored reduction provides a speedup of 3% in signing. Additionally, our implementation of Tailored reduction using AVX-512IFMA is much faster than AVX-512F, confirming that IFMA does indeed improve the performance of Tailored reduction implementation.

Operation	Impl.	CPU cycles
Sign-original	AVX-512	239244
Sign-opt1	AVX-512F	234124
Sign-opt2	AVX-512IFMA	231962

**TABLE V:** Comparative performance of Tailored Reduction in Dilithium2(Cycles).

### B. PSPM-TEE Performance

Table VI shows the performance of the Improved PSPM algorithm. By applying Improved PSPM, our AVX2 implementation obtains a speedup of about 9% in Dilithium3. Dilithium5 has the least acceleration, only 2.6%. The results clearly show that the improved PSPM benefits to the Signing procedure of Dilithium. So we use the improved PSPM algorithm in implementing Dilithium using AVX512 as well.

	AVX2	AVX2 (PSPM – TEE)	Speedup
Dilithium2	254922	231766	9.0%
Dilithium3	407316	393454	3.4%
Dilithium5	514992	501304	2.6%

**TABLE VI:** Performance of Signing Procedure with Improved PSPM (Cycles).

### C. Other Vectorization Functions Performance

We conducted an experiment to primarily test the performance of our AVX-512 vectorized functions in Dilithium. We tested three sampling functions: `poly_uniform`, `poly_uniform_eta`, and `poly_uniform_gamma1`. Overall, polynomial sampling can bring about a three to four-fold increase in performance. This improvement mainly comes from the hash and rejection sampling functions, where `poly_uniform` and `poly_uniform_eta` use `SHAKE-128` hash function, and `poly_uniform_gamma1` uses `SHAKE-256`. To obtain further performance data, we separately tested the speed of rejection sampling and hashing. According to Table IX in Appendix A, the 8-way `poly_uniform` implementation's primary performance improvement comes from the 5.5-fold improvement of `SHAKE-128`, with the help of 16-way rejection sampling which has a 5.63-fold improvement. However, since the polynomial sampling part is not entirely 8-way, when sampling less than 16 polynomial coefficients, the 1-way polynomial sampling is still used, so the final performance improvement does not fully reach a five-fold speedup, and the other two sampling functions remain the same. Our 16-way `rej_uniform` and `rej_eta` implementation can achieve a five to six-fold speedup overall. However, the speedup is somewhat limited, mainly because the rejection sampling part requires some shuffle operations to ensure the correctness of the test vectors, and the rejection sampling process is not entirely vectorizable.

For the NTT part, we utilized a compact method for loading coefficients, allowing us to load 16 coefficients at once instead of the AVX2's load of four coefficients at a time. As a result, we were able to achieve 16-way parallelism in the NTT part. This allowed us to achieve a significant acceleration ratio of almost 14 times in the NTT operation. Similarly, in the inverse NTT implementation, we were able to achieve a speedup of almost 18 times. The acceleration of the NTT part mainly comes from the vectorization of AVX-512 itself, as well as our reasonable instruction schedule and full utilization of registers, reducing load and store operations through layer merging technology.

In the polynomial pointwise multiplication function, the parallelism is reduced by half during the calculation due to the large number of  $32bits \times 32bits \Rightarrow 64bits$  multiplication operations, resulting in only an 11-fold acceleration ratio. We also implemented AVX-512's 64-way vectorization on the packing part, and the corresponding data is shown in Table IX in Appendix A. However, since Dilithium's AVX2 code does not have a `polyz_unpack` implementation, the 32-way data is not given here. Our 16-way vectorization achieves a 30-fold speedup. The main bottleneck of the `polyz_unpack` acceleration is the coefficient's reordering to ensure the correctness of the test vectors. The `polyw1_pack` itself is relatively simple. The C implementation is already fast, so the 16-way implementation does not bring much acceleration.

### D. Scheme Performance

In this work, to give the best performance, we apply various optimization techniques to Dilithium implementation, including optimized implementations in NTT, rejection sampling, decomposing and computing hints, bit-packing, and so on. Table VIII summarizes the cycle counts and comparisons for all three security levels of Dilithium, including key generation (KeyGen), signing (Sign), and verification (Verify).

We enhanced our previous AVX2 implementation by using improved PSPM and tailored reduction, resulting in a speedup of 3% to 9% in the signature procedure. In our implementation of Dilithium AVX-512, there are some parts that have not yet been vectorized, such as hash functions other than polynomial sampling. Therefore, the overall improvement in signature speed cannot exceed twice the AVX2 software speed. However, our speedup is mainly attributed to the vectorization of certain functions and optimization techniques that we have introduced.

**TABLE VII:** Performance comparison in Signing procedure (Cycles).

Scheme	AVX2 [13]	AVX2 (Our work)	Speedup
Dilithium2	254922	231410	9.22%
Dilithium3	407316	392436	3.65%
Dilithium5	514992	500882	2.74%

### E. Discussions about Side-Channel Security and Memory Cost

Constant-time implementation (CTI) was not the focus of this work, but we indeed take it in mind. We have carefully

**TABLE VIII:** Execution times (in Cycles) of implementation of Dilithium2, Dilithium3 and Dilithium5 on an Intel Core i7-11700F processor.

Scheme	Operation	C [13]	AVX2 [13]	AVX-512		
		Cycles	Cycles	Cycles	Speedup vs C	Speedup vs AVX2
Dilithium2	KeyGen	266772	106000	66432	75.1%	37.3 %
	Sign	1033894	251050	165532	83.9%	34.1%
	Verify	298384	107338	66396	77.7%	38.1%
Dilithium3	KeyGen	503306	246988	121766	75.8%	50.7%
	Sign	1699294	406248	255508	84.9%	37.1%
	Verify	478660	174218	106664	77.7%	38.7%
Dilithium5	KeyGen	725802	286534	172782	76.1%	39.7%
	Sign	2111234	516200	295740	86.0%	42.7%
	Verify	770794	275894	163486	78.8%	40.7%

avoided using branching statements depending on secret information, and we have not used the modulo operator %. For the side-channel security of the PSPM-TEE technique, we have the following observations. On the one hand, as the intermediate hashing  $c$ 's rejected with the tailored early evaluation are never output, the intermediate values are actually blinded to an outside observer. On the other hand, the PSPM technique combines the same dimension coefficient of multiple small polynomials into one word to operate, which could make more difficulties or obstacle for side-channel attacks than traditional NTT techniques.

For space cost, our implementation pre-calculates the tables in improved PSPM, which requires an additional 8192 bytes of storage space in Dilithium3/5 and 4096 bytes in Dilithium2. However, our implementation of parallel rejection sampling saves 1048576 bytes. Overall, our implementation significantly reduces the required space compared to the previous AVX2 implementations.

## REFERENCES

- [1] X. . ITU-T Recommendation, "Information technology-open systems interconnection-the directory: public-key and attribute certificate framework," *ISO/IEC 9594-8: 2001*, 2000.
- [2] T. Dierks and E. Rescorla, "The transport layer security (TLS) protocol version 1.2," Tech. Rep., 2008.
- [3] E. Rescorla, "The transport layer security (TLS) protocol version 1.3," Tech. Rep., 2018.
- [4] R. L. Rivest, A. Shamir, and L. Adleman, "A method for obtaining digital signatures and public-key cryptosystems," *Communications of the ACM*, vol. 21, no. 2, pp. 120–126, 1978.
- [5] P. W. Shor, "Polynomial-time algorithms for prime factorization and discrete logarithms on a quantum computer," *SIAM review*, vol. 41, no. 2, pp. 303–332, 1999.
- [6] K. McKay, L. Bassham, M. Sönmez Turan, and N. Mouha, "Report on lightweight cryptography," National Institute of Standards and Technology, Tech. Rep., 2016.
- [7] G. Alagic, D. Apon, D. Cooper, Q. Dang, T. Dang, J. Kelsey, J. Lichtinger, C. Miller, D. Moody, R. Peralta *et al.*, "Status report on the third round of the NIST post-quantum cryptography standardization process," *US Department of Commerce, NIST*, 2022.
- [8] A. Langlois and D. Stehlé, "Worst-case to average-case reductions for module lattices," *Des. Codes Cryptogr.*, vol. 75, no. 3, pp. 565–599, 2015. [Online]. Available: <https://doi.org/10.1007/s10623-014-9938-4>
- [9] M. Ajtai, "Generating hard instances of lattice problems," in *Proceedings of the twenty-eighth annual ACM symposium on Theory of computing*, 1996, pp. 99–108.
- [10] V. Lyubashevsky, "Fiat-shamir with aborts: applications to lattice and factoring-based signatures," in *International Conference on the Theory and Application of Cryptology and Information Security*. Springer, 2009, pp. 598–616.
- [11] C. Lomont, "Introduction to intel advanced vector extensions," *Intel white paper*, vol. 23, 2011.
- [12] I. Corporation, "10th generation intel core processor based on ice lake microarchitecture instruction throughput and latency." Available online at <https://software.intel.com/content/www/us/en/develop/download/10th-generation-intel-core-processor-instruction-throughput-and-latency-docs.html>, 2020.
- [13] R. Avanzi, J. Bos, and L. Ducas, "Submission to the NIST post-quantum cryptography standardization project," Available for download at <https://csrc.nist.gov/CSRC/media/Projects/post-quantum-cryptography/documents/round-3/submissions/Dilithium-Round3.zip>, 2022.
- [14] D. O. C. Greconici, M. J. Kannwischer, and D. Sprenkels, "Compact Dilithium implementations on Cortex-M3 and Cortex-M4," *IACR Trans. Cryptogr. Hardw. Embed. Syst.*, vol. 2021, no. 1, pp. 1–24, 2021. [Online]. Available: <https://doi.org/10.46586/tches.v2021.i1.1-24>
- [15] Y. Kim, J. Song, T.-Y. Youn, and S. C. Seo, "CRYSTALS-Dilithium on ARMv8," *Security and Communication Networks*, vol. 2022, 2022.
- [16] H. Becker, V. Hwang, M. J. Kannwischer, B. Yang, and S. Yang, "Neon NTT: faster Dilithium, Kyber, and Saber on Cortex-A72 and Apple M1," *IACR Trans. Cryptogr. Hardw. Embed. Syst.*, vol. 2022, no. 1, pp. 221–244, 2022. [Online]. Available: <https://doi.org/10.46586/tches.v2022.i1.221-244>
- [17] A. Abdulrahman, V. Hwang, M. J. Kannwischer, and D. Sprenkels, "Faster Kyber and Dilithium on the Cortex-M4," in *Applied Cryptography and Network Security - 20th International Conference, ACNS 2022, Rome, Italy, June 20-23, 2022, Proceedings*, ser. Lecture Notes in Computer Science, G. Ateniese and D. Venturi, Eds., vol. 13269. Springer, 2022, pp. 853–871. [Online]. Available: [https://doi.org/10.1007/978-3-031-09234-3\\_42](https://doi.org/10.1007/978-3-031-09234-3_42)
- [18] J. Bradbury and B. Hess, "Fast quantum-safe cryptography on IBM Z." Technical report, 2021. URL: <https://csrc.nist.gov/CSRC/media/Event/s/third-pqc-standardization-conference/documents/accepted-papers/hess-fast-quantum-safe-pqc2021.pdf>, 2021.
- [19] J. Zheng, F. He, S. Shen, C. Xue, and Y. Zhao, "Parallel small polynomial multiplication for dilithium: a faster design and implementation," in *Annual Computer Security Applications Conference, ACSAC 2022, Austin, TX, USA, December 5-9, 2022*. ACM, 2022, pp. 304–317. [Online]. Available: <https://doi.org/10.1145/3564625.3564629>
- [20] J. W. Bos, P. L. Montgomery, D. Shumow, and G. M. Zaverucha, "Montgomery multiplication using vector instructions," in *International Conference on Selected Areas in Cryptography*. Springer, 2014, pp. 471–489.
- [21] S. Gueron and F. Schlieker, "Speeding up R-LWE post-quantum key exchange," in *Nordic conference on secure IT systems*. Springer, 2016, pp. 187–198.
- [22] G. Orisaka, D. F. Aranha, and J. López, "Finite field arithmetic using AVX-512 for isogeny-based cryptography," in *Anais do XVIII Simpósio Brasileiro de Segurança da Informação e de Sistemas Computacionais*. SBC, 2018, pp. 49–56.
- [23] T. Edamatsu and D. Takahashi, "Acceleration of large integer multiplication with intel AVX-512 instructions," in *20th IEEE International Conference on High Performance Computing and Communications; 16th IEEE International Conference on Smart City; 4th IEEE International Conference on Data Science and Systems, HPCC/SmartCity/DSS 2018, Exeter, United Kingdom, June 28-30, 2018*. IEEE, 2018, pp. 211–218. [Online]. Available: <https://doi.org/10.1109/HPCC/SmartCity/DSS.2018.00059>
- [24] D. Takahashi, "An implementation of parallel number-theoretic transform using Intel AVX-512 instructions," in *International Workshop on Computer Algebra in Scientific Computing*. Springer, 2022, pp. 318–332.
- [25] J. Robert and P. Véron, "Faster multiplication over  $\mathbb{F}_2[x]$  using AVX512 instruction set and VPCLMULQDQ instruction," *CoRR*, vol. abs/2201.10473, 2022. [Online]. Available: <https://arxiv.org/abs/2201.10473>
- [26] H. Cheng, G. Fotiadis, J. Großschädl, and P. Y. A. Ryan, "Highly vectorized SIKE for AVX-512," *IACR Trans. Cryptogr. Hardw. Embed. Syst.*, vol. 2022, no. 2, pp. 41–68, 2022. [Online]. Available: <https://doi.org/10.46586/tches.v2022.i2.41-68>
- [27] H. Cheng, G. Fotiadis, J. Großschädl, P. Y. A. Ryan, and P. B. Rønne, "Batching CSIDH group actions using AVX-512," *IACR Trans. Cryptogr. Hardw. Embed. Syst.*, vol. 2021, no. 4, pp. 618–649, 2021. [Online]. Available: <https://doi.org/10.46586/tches.v2021.i4.618-649>
- [28] D. M. Alter, "Optimizing the NIST post quantum candidate SPHINCS+ using AVX-512," <https://github.com/DorAlter/sphincsplus/tree/avx512-i> mplementation, 2021.
- [29] R. Cabral and J. López, "Implementation of the SHA-3 family using AVX512 instructions," in *Anais do XVIII Simpósio Brasileiro de*

*Segurança da Informação e de Sistemas Computacionais*. SBC, 2018, pp. 25–32.

- [30] S. Bai, L. Ducas, E. Kiltz, T. Lepoint, V. Lyubashevsky, P. Schwabe, G. Seiler, and D. Stehlé, “CRYSTALS-Dilithium algorithm specifications and supporting documentation (version 3.1),” *NIST Post-Quantum Cryptography Standardization Round*, vol. 3, 2021.
- [31] M. J. Dworkin *et al.*, “SHA-3 standard: permutation-based hash and extendable-output functions,” 2015.
- [32] G. Seiler, “Faster AVX2 optimized NTT multiplication for ring-lwe lattice cryptography,” *IACR Cryptol. ePrint Arch.*, p. 39, 2018. [Online]. Available: <http://eprint.iacr.org/2018/039>
- [33] J. W. Cooley and J. W. Tukey, “An algorithm for the machine calculation of complex fourier series,” *Mathematics of computation*, vol. 19, no. 90, pp. 297–301, 1965.
- [34] W. M. Gentleman and G. Sande, “Fast fourier transforms: for fun and profit,” in *Proceedings of the November 7-10, 1966, fall joint computer conference*, 1966, pp. 563–578.

## APPENDIX

### A. PSPM with Early Evaluation pseudocode for Dilithium3/5

**Algorithm 11** A parallel index-based polynomial multiplication algorithm with early evaluating  $\mathbf{z}$  for Dilithium3/5

**Input:**  $(c, \mathbf{s}, \mathbf{y})$ , where  $\mathbf{s} = [s^{(0)}, \dots, s^{(l-1)}]^T \in \mathcal{R}_q^l, \mathbf{y} \in \mathcal{R}_q^l$ , every  $s^{(j)} = \sum_{i=0}^{n-1} s_i^{(j)} \cdot x^i \in \mathcal{R}_q, y^{(j)} = \sum_{i=0}^{n-1} y_i^{(j)} \cdot x^i \in \mathcal{R}_q$ , and  $c = \sum_{i=0}^{n-1} c_i \cdot x^i \in \mathcal{B}_\tau$

**Output:**  $\mathbf{z} = c \cdot \mathbf{s} + \mathbf{y} = [z^{(0)}, \dots, z^{(l-1)}]^T \in \mathcal{R}_q^l$ , where  $z^{(j)} = c \cdot s^{(j)} + y^{(j)} = \sum_{i=0}^{n-1} z_i^{(j)} \cdot x^i \in \mathcal{R}_q$

```

1: for  $i \in \{0, 1, \dots, n-1\}$  do
2:    $m_i := 0$ 
3:    $v_i := 0$ 
4:    $v_{i-n} := 0$ 
5:   for  $j \in (0, 1, \dots, l-1)$  do
6:      $v_i := v_i \cdot M + (U + s_i^{(j)})$ 
7:      $v_{i-n} := v_{i-n} \cdot M + (U - s_i^{(j)})$ 
8:    $\gamma := 2U \cdot \frac{M^l - 1}{M - 1}$ 
9:   for  $i \in \{0, 1, \dots, n-1\}$  do
10:    if  $c_i = 1$  then
11:      for  $j \in \{0, 1, \dots, n-1\}$  do
12:         $m_j := m_j + v_{j-i}$ 
13:    if  $c_i = -1$  then
14:      for  $j \in \{0, 1, \dots, n-1\}$  do
15:         $m_j := m_j + (\gamma - v_{j-i})$ 
16:   for  $i \in \{0, 1, \dots, n-1\}$  do
17:      $t := m_i$ 
18:     for  $j \in (0, 1, \dots, l-1)$  do
19:        $z_i^{(l-1-j)} := (t \bmod M) - \tau U \pmod{q}$ 
20:        $z_i^{(l-1-j)} := z_i^{(l-1-j)} + y_i^{(l-1-j)}$ 
21:       if  $|z_i^{(l-1-j)}| \geq \gamma_1 - \beta$  then Restart signature process.
22:      $t := \lfloor t/M \rfloor$ 
23: return  $\mathbf{z} = [z^{(0)}, \dots, z^{(l-1)}]^T$ 

```

### B. Benchmark Results for Vectorization Functions

Function	Vectorization	Cycles	Speedup
Poly_uniform	1-way	5784	1.00x
	4-way	19488	2.97x
	8-way	13450	4.30x
Poly_uniform_eta	1-way	30158	1.00x
	4-way	17858	1.69x
	8-way	9054	3.33x
Poly_uniform_gamma1	1-way	48148	1.00x
	4-way	24594	1.95x
	8-way	12094	3.98x
SHAKE-256	1-way	5934	1.00x
	4-way	2896	2.05x
	8-way	1014	5.85x
SHAKE-128	1-way	6126	1.00x
	4-way	3006	2.04x
	8-way	1114	5.50x
rej_uniform	1-way	450	1.00x
	8-way	230	1.96x
	16-way	80	5.63x
rej_eta	1-way	1122	1.00x
	8-way	322	3.48x
	16-way	230	4.88x
NTT	1-way	6896	1.00x
	4-way	1326	5.00x
	16-way	494	13.95x
NTT <sup>-1</sup>	1-way	9438	1.00x
	4-way	1090	8.66x
	16-way	526	17.94x
poly_pointwise	1-way	1374	1.00x
	4-way	146	9.41x
	16-way	124	11.08x
polyz_unpack	1-way	962	1.00x
	32-way	-	-
	64-way	32	30x
polyw1_pack	1-way	32	1.00x
	8-way	32	1.00x
	16-way	16	2.00x

**TABLE IX:** Experimental results of vectorization functions for Dilithium (Cycles).

### C. Parameter for PSPM

**TABLE X:** Parallel Parameters of Dilithium.

Scheme	Operation	$\tau$	$U$	$2\tau U$	M	$r$
Dilithium2	cs <sub>1</sub>	39	2	156	2 <sup>8</sup>	4
	cs <sub>2</sub>	39	2	156	2 <sup>8</sup>	4
	ct <sub>0</sub>	39	2 <sup>12</sup>	319488	2 <sup>19</sup>	4
	ct <sub>1</sub>	39	2 <sup>10</sup>	79872	2 <sup>17</sup>	4
Dilithium3	cs <sub>1</sub>	49	4	392	2 <sup>9</sup>	5
	cs <sub>2</sub>	49	4	392	2 <sup>9</sup>	6
	ct <sub>0</sub>	49	2 <sup>12</sup>	401408	2 <sup>19</sup>	6
	ct <sub>1</sub>	49	2 <sup>10</sup>	100352	2 <sup>17</sup>	6
Dilithium5	cs <sub>1</sub>	60	2	240	2 <sup>8</sup>	7
	cs <sub>2</sub>	60	2	240	2 <sup>8</sup>	8
	ct <sub>0</sub>	60	2 <sup>12</sup>	491520	2 <sup>19</sup>	8
	ct <sub>1</sub>	60	2 <sup>10</sup>	122880	2 <sup>17</sup>	8